ISSN 2176-5480

22nd International Congress of Mechanical Engineering (COBEM 2013)
November 3-7, 2013, Ribeirão Preto, SP, Brazil

ENTROPY GENERATION MINIMIZATION ANALYSIS OF PASSIVE REGENERATORS

Paulo V. Trevizoli
Diego P. Alcalde
Jader R. Barbosa Jr.
POLO - Research Laboratories for Emerging Technologies in Cooling and Thermophysics, Department of Mechanical Engineering, Federal University of Santa Catarina, Florianópolis, SC, 88040-900, Brazil
E-mail: trevizoli@polo.ufsc.br
E-mail: dpalcalde@polo.ufsc.br
E-mail: jrb@polo.ufsc.br

Abstract. *The thermodynamic efficiencies of active and passive regenerative cooling cycles are directly linked to the heat transfer effectiveness and thermal losses taking place in the regenerator. This paper proposes an optimization method for regenerators based on the Entropy Generation Minimization (EGM) method. The model consists of the one-dimensional Brinkman-Forchheimer equation to describe the fluid flow and coupled energy equations for the fluid and solid phases. An equation is proposed to determine the entropy generation contributions due to axial heat conduction, fluid friction and interstitial heat transfer. The influence of parameters such as the mass flow rate, regenerator cross sectional area, housing aspect ratio, utilization factor and particle diameter was evaluated in the context of Variable Geometry and Fixed Face Area Performance Evaluation Criteria (PEC). Optimal regenerator configurations were found for each PEC for flow rates between* 50 *and* 200 *kg/h with constraints of regenerator effectiveness equal to 95%.*

Keywords: *passive regenerator, porous media, entropy generation minimization (EGM)*

1. INTRODUCTION

Regenerators are storage-type heat exchangers where hot and cold fluid streams flow in alternating directions through a porous matrix, giving rise to intermittent heat transfer between the solid and the fluid. During a hot blow, the fluid at a higher temperature exchanges heat with the solid phase, warming up the matrix that stores thermal energy from the fluid phase. In the cold blow, the matrix releases the stored energy as heat, warming up the fluid (Schmidt and Willmott, 1981; Shah and Sekulic, 2003). Regenerators are widely employed in power and cooling gas cycles such as the Stirling, pulse-tube, thermoacoustic, Gifford-McMahon and Vuillemier cycles. Regenerators that use liquids as a working fluid are encountered in some magnetic cooling cycles. In these cases, such as in the Brayton magnetic cooling cycle, the regenerator can be classified as *active*, since the solid matrix is made of a magnetocaloric material that is heated up or cooled down (with respect to the ambient temperature) when the regenerator is magnetized or demagnetized adiabatically (Pecharsky and Gschneidner, 1999).

In active magnetocaloric regenerators, the structure and geometry of the solid matrix are very important for establishing desirable values of temperature span and cycle efficiency. An ideal regenerative matrix geometry is one with large thermal mass, surface area and thermal conductance, but negligible viscous losses. Due to the sometimes prohibitive manufacturing and processing costs of magnetocaloric materials, it is not always possible to make systematic experimental evaluations of different geometries of the solid matrix. Nevertheless, experiments with non-magnetic solid matrices may help in the quantification of the influence of the porous medium geometry on the thermal-hydraulic performance of the regenerator separately from thermodynamic losses related to magnetic phenomena in the matrix (Trevizoli *et al.*, 2012).

A regenerator can be designed and optimized based on the Entropy Generation Minimization (EGM) method. This method has been developed to evaluate the thermodynamic performance of thermal systems based on the irreversibilities due to heat transfer and fluid friction. Bejan (1982, 1996) presented several applications of the method in the context of heat exchangers and storage systems. A recent review was presented by Awad and Muzychka (2012). Krane (1987) evaluated the performance of regenerators using gases as working fluids and concluded that the storage and removal processes need to be analyzed together in order to determine the optimum characteristics of these devices, which were observed to be quite inneficient (i.e., 70-90% of the available exergy is destroyed by the end of a cycle). Das and Sahoo (1991) used the EGM method in the thermodynamic optimization of regenerators under single blow operation (i.e., no time dependence). Their model disregarded axial heat conduction and was valid only for $0 < NTU \leq 7$. An optimum operating condition was identified in terms of the cycle time and NTU. In a subsequent work, Das and Sahoo (1999) included the time dependence and the axial conduction in the EGM analysis, thus extending the validity of their model to more densely packed regenerators operating at higher values of NTU.

de Waele *et al.* (1997) and Steijaert (1999) applied the EGM method to pulse-tube cryocoolers, taking into consider-

ISSN 2176-5480

ation the entropy production in all of the pulse-tube device components (orifice, heat exchangers, regenerator, switching valves). The model was used to evaluate the thermodynamic performance of a cryocooler prototype. Based on the work of de Waele *et al.* (1997), Nam and Jeong (2006) employed the EGM method in the analysis of parallel wire (segmented and unsegmented) mesh regenerators. They observed a better performance of the unsegmented parallel wire configuration, in comparison to a screen mesh matrix, due to lower porosity and hence friction factor. However, axial heat conduction was identified as the main source of irreversibility in the parallel wire case. To overcome this loss, a segmented parallel wire geometry was used to decrease the axial conduction irreversibility and improve the thermodynamic performance of the parallel wire regenerator.

The present work proposes a methodology based on the EGM method to design optimal thermal passive regenerators. The mathematical model is composed of the one-dimensional Brinkman-Forchheimer equation for momentum transfer in porous media coupled with energy balance equations for the fluid and solid phases. The local instantaneous velocity and temperature fields are used in the calculation of the local rates of entropy generation per unit volume due to (i) fluid friction, (ii) axial heat conduction in both media and (iii) interstitial heat transfer with a finite temperature difference between the phases. Since the ultimate application for the present methodology will involve the optimization of active magnetic regenerators, the working fluid has been treated as a liquid (aqueous solution). As performed by Pussoli *et al.* (2012) in the optimization of peripheral-finned tube recuperators, the total entropy generation, S_g, was used as the objective function in an optimization procedure which makes used of the Performance Evaluation Criteria (PEC) proposed by Webb and Kim (2005). In these PEC, the heat exchange device can be optimized according to fixed volume, fixed face area or variable geometry constraints, which may be useful in the context of regenerator design for both passive and active applications.

2. MATHEMATICAL MODELING

The mathematical model for the thermal-hydraulic analysis of passive regenerators is based on a similar model for active magnetic regenerators (Trevizoli *et al.*, 2013). The following simplifying assumptions have been adopted: one-dimensional, laminar and incompressible fluid flow, low porosity porous medium ($\varepsilon < 0.6$) and absence of body forces.

2.1 Fluid Flow Model

The Brinkman-Frochheimer equation for momentum transfer in porous media is given by (Kaviany, 1995; Nield and Bejan, 2006),

$$\frac{\rho_f}{\varepsilon}\left(\frac{\partial \vec{v}}{\partial t} + \vec{v}\cdot\nabla\vec{v}\right) = -\nabla p + \rho_f \vec{f} + \frac{\mu_f}{\varepsilon\rho_f}\nabla^2\vec{v} - \frac{\mu_f}{K}\vec{v} - \frac{c_E\rho_f}{K^{1/2}}|\vec{v}|\vec{v} \tag{1}$$

where the term on the left hand side is the macroscopic inertial force and those on the right hand side are the pore pressure gradient, the body force, the macroscopic viscous shear stress (or Brinkman viscous term), the microscopic shear stress (or Darcy term) and the microscopic inertial force (or Ergun inertial term), respectively. Assuming simplifying assumptions one has,

$$\frac{\rho_f}{\varepsilon}\left(\frac{\partial u}{\partial t}\right) = -\frac{\partial p}{\partial z} - \frac{\mu_f}{K}u - \frac{c_E\rho_f}{K^{1/2}}|u|u \tag{2}$$

where u is the Darcian (superficial) velocity, t is time, p is the pressure, ρ_f is the fluid density, μ_f is the fluid kinematic viscosity, ε is the porosity, z is the axial distance, D_p is the particle diameter and D_h is the regenerator housing hydraulic diameter based on the cross sectional area. $K = \varepsilon^3 D_p/180(1-\varepsilon)^2$ is the permeability of the porous media and $C_E = 0.55(1 - 5.5D_p/D_h)$ is the Ergun constant. In dimensionless form, Eq. 2 is given by,

$$\frac{Re_\omega Da}{\varepsilon}\frac{\partial u^*}{\partial t^*} = -g(t^*) - u^* - C|u^*|u^* \tag{3}$$

where $t^* = \omega t$, $\omega = 2\pi f$ is the angular frequency and f the cycle frequency. To describe the oscillatory flow in a regenerator, the pressure gradient was approximated by a time dependent waveform as follows (Zhao and Cheng, 1996, 1998; Oliveira *et al.*, 2012),

$$-\frac{\partial p}{\partial z} = \rho_f A_t g(t^*) \tag{4}$$

where A_t is the amplitude of the fluid flow waveform and $g(t^*)$ is a wave function. For a sinusoidal waveform, $g(t^*) = \sin(\omega t)$. The dimensionless pressure gradient is given by,

ISSN 2176-5480

$$-\frac{\partial p}{\partial z}\Big|^{*} = g(t^{*}) \tag{5}$$

The dimensionless velocity is defined as $u^{*} = u/u_{D,max}$, where $u_{D,max}$ is the maximum Darcy velocity calculated directly by the classical Darcy Equation for which $g(t^{*})$ is by definition equal to unity. Thus,

$$u_{D,max} = -\frac{K}{\mu_f}\frac{\partial p}{\partial z}\Big|_{max} = -\frac{K}{\nu_f}A_t \tag{6}$$

where ν_f is the kinematic viscosity of the fluid. The dimensionless groups in Eq. (3) are the kinetic Reynolds number $Re_\omega = \omega d_h^2/\nu_f$, the Darcy number $Da = K/d_h^2$ and $C = C_E A_t K^{1.5}/\nu_f^2$. d_h is the porous media hydraulic diameter calculated by $d_h = 4\varepsilon/\beta$, where β is the surface area density of the porous medium. It should be noted that, when terms other than the microscopic shear stress are non-negligible, the actual maximum velocity in the channel (u_{max}) is different from $u_{D,max}$, which means that the value of u_D^{*} will be less than unity (Trevizoli *et al.*, 2013).

2.2 Heat Transfer Model

The energy equation for the one-dimensional, laminar, incompressible fluid flow is given by,

$$\varepsilon\frac{\partial T_f}{\partial t} = -\frac{\hbar\beta}{\rho_f c_{p,f}}(T_f - T_s) - u\frac{\partial T_f}{\partial z} + \varepsilon\frac{\kappa_d}{\rho_f c_{p,f}}\frac{\partial^2 T_f}{\partial z^2} + \frac{1}{\rho_f c_{p,f}}\left|\frac{\partial p}{\partial z}u\right| \tag{7}$$

where the term on the left is due to inertial (thermal capacity) effects and those on the right are the transversal heat transfer term calculated using a convective heat transfer coefficient, the longitudinal advection term, the axial conduction term and the viscous dissipation term. T_f is the fluid temperature, T_s is the solid temperature, $\hbar$ is the convective heat transfer coefficient, β is the surface area density, $c_{p,f}$ is the fluid heat capacity. $\kappa_d = k_f(1 + D_f)$ is the thermal conductivity corrected by the dispersion contribution, where k_f is the fluid thermal conduction and $D_f = 0.75Pe_R$ is the longitudinal thermal dispersion for a packed bed of spheres, for $Pe_R >> 1$. $Pe_R = Re_R Pr$ is the Peclet number, Re_R is the Reynolds number based on the particle radious and Pr the Prandtl number (Koch and Brady, 1985; Kaviany, 1995). In dimensionless form, Eq. (7) is given by,

$$\frac{\partial\theta_f}{\partial t^{*}} = -NuFo_f(\theta_f - \theta_s) - \frac{Re_{max}}{Re_\omega\zeta_r}u^{*}\frac{\partial\theta_f}{\partial z^{*}} + \frac{1}{\gamma_d Pr Re_\omega\zeta_r^2}\frac{\partial^2\theta_f}{\partial z^{*2}} + \frac{Br}{Pr}\left|f(t^{*})u^{*}\right| \tag{8}$$

where the dimensionless fluid and solid temperatures are given by $\theta_{f,s} = (T_{f,s} - T_{CHEX})/(T_{HHEX} - T_{CHEX})$, where T_{CHEX} and T_{HHEX} are the cold and hot source temperatures, respectively. $u^{*} = u/u_{max}$ (where u_{max} is the actual maximum velocity in the oscillatory flow field. $z^{*} = z/L$ is the dimensionless distance, where L is the length of the regenerator bed. In Eq. (8), the dimensionless groups are the interstitial Nusselt number, $Nu = \hbar d_h/k_f$, maximum velocity Reynolds number, $Re_{max} = \left(\frac{u_{max}}{\varepsilon}\right)\left(\frac{d_h}{\nu_f}\right)$, Brinkman number $Br = \mu_f A_t\frac{u_{max}}{\varepsilon}/k_f\omega(T_{HHEX} - T_{CHEX})$ and Fourier number of the fluid phase, $Fo_f = \frac{\alpha_f}{\omega}\Big/\left(\frac{d_h}{2}\right)^2$, where α_f is the thermal diffusivity of the fluid. The aspect ratio is defined as $\zeta_r = L/d_h$ and the thermal conductivity ratio is given by $\gamma_d = \kappa_d/k_f$. The interstitial Nusselt number for the packed bed of spheres was calculated using the Whitaker correlation (Kaviany, 2002).

The energy equation for the solid phase is given by,

$$(1-\varepsilon)\frac{\partial T_s}{\partial t} = -\frac{\hbar\beta}{\rho_s c_s}(T_s - T_f) + (1-\varepsilon)\frac{\kappa_{stc}}{\rho_s c_s}\frac{\partial^2 T_s}{\partial z^2} \tag{9}$$

where the term on the left accounts for thermal inertia in the solid, and those on the right are the transversal heat transfer term due to interstitial heat convection and axial heat conduction term. ρ_s is the solid density, c_s is the solid specific heat and κ_{stc} is the static thermal conductivity calculated by the Hadley correlation (Hadley, 1986; Kaviany, 1995). Using the same dimensionless variables, the dimensionless energy equation for the solid phase is given by,

$$\frac{\partial\theta_s}{\partial t^{*}} = -BiFo_s(\theta_s - \theta_f) + \frac{\alpha^{*}}{\gamma_{stc}Pr Re_\omega\zeta_r^2}\frac{\partial^2\theta_s}{\partial z^{*2}} \tag{10}$$

where $\gamma_{stc} = k_s/\kappa_{stc}$ is the thermal conductivity ratio, $\alpha^{*} = \alpha_s/\alpha_f$ is the thermal diffusivity ratio, $Bi = \hbar d_h/k_s$ is the Biot number and $Fo_s = \alpha_s/\omega\ell_c^2$, where $\ell_c = (1-\varepsilon)/\beta$ is the characteristic length of the porous medium (Trevizoli *et al.*, 2013).

ISSN 2176-5480

2.3 Entropy generation

The entropy production in the one-dimensional passive regenerator model is due to heat transfer between solid and fluid phases, axial heat conduction in the fluid and solid phases and viscous dissipation in the fluid. Therefore, the rate of entropy change in a control volume containing both the solid and fluid phases is given by (Steijaert, 1999),

$$\left.\frac{dS}{dt}\right|_{CV} = -(1-\varepsilon)A_c\left[\frac{d}{dz}\left(\frac{q''_{AC,s}}{T_s}\right)dz\right]_s - \varepsilon A_c\left[\frac{d}{dz}\left(\frac{q''_{AC,f}}{T_f}\right)dz\right]_f + \dot{m}\frac{ds}{dz}dz + S'''_g A_c dz \tag{11}$$

where the first and second terms on the right are changes in entropy rate due to axial conduction heat transfer in the solid and fluid. The third term is the rate of entropy change associated with the fluid flow into and out of the control volume. The fourth term is the rate of entropy generation in the control volume. The rate of entropy change in the control volume is the sum of the entropy changes in the fluid and solid phases,

$$\left.\frac{dS}{dt}\right|_{CV} = \left.\frac{dS}{dt}\right|_f + \left.\frac{dS}{dt}\right|_s \tag{12}$$

where the rates of entropy change in the fluid and solid are given by (Steijaert, 1999),

$$\left.\frac{dS}{dt}\right|_f = -\frac{\varepsilon A_c}{T_f}\left[\frac{dq''_{AC,f}}{dz}dz\right]_f + \frac{q''_{HT}}{T_f}A_c dz + \dot{m}\frac{ds}{dz}dz + \frac{1}{\rho_f T_f}\left|\dot{m}\left(-\frac{dp}{dz}\right)\right|dz \tag{13}$$

$$\left.\frac{dS}{dt}\right|_s = -\frac{(1-\varepsilon)A_c}{T_s}\left[\frac{dq''_{AC,s}}{dz}dz\right]_s - \frac{q''_{HT}}{T_s}A_c dz \tag{14}$$

where $q''_{AC,f} = -\kappa_d dT_f/dz$ and $q''_{AC,s} = -\kappa_{stc} dT_s/dz$ are the axial heat fluxes in the liquid and solid domains. $q''_{HT} = \hbar\beta(T_s - T_f)$ is the heat transfer rate per unit surface area between the fluid and solid phases, where $\hbar$ is the interstitial convective heat transfer coefficient.

Combining Eqs. (11)-(14) and Eq. (12), the local rate of entropy generation per unit volume is given by,

$$\dot{S}'''_g = \frac{\hbar\beta(T_s - T_f)^2}{T_s T_f} + \frac{\varepsilon\kappa_f}{T_f^2}\left(\frac{dT_f}{dz}\right)^2 + \frac{(1-\varepsilon)\kappa_{stc}}{T_s^2}\left(\frac{dT_s}{dz}\right)^2 + \frac{1}{T_f}\left|u_D\left(-\frac{dp}{dz}\right)\right| \tag{15}$$

where the first term on the right is the entropy generation rate per unit volume due to interphase heat transfer with a finite temperature difference. The second and third terms are the entropy generation rate due to axial conduction in the fluid and solid matrix, and the fourth term is the entropy generation rate per unit volume due to viscous friction. The entropy generation in the regenerator during a cycle, S_g, is calculated by (in J/K),

$$S_g = A_c\int_0^L\int_0^\tau \dot{S}'''_g\, dt\, dz \tag{16}$$

S_g will be used as the objective function to be minimized in the regenerator optimization described next.

2.4 Performance evaluation criteria

The simulations for the entropy generation minimization were carried out based on performance evaluation criteria (PEC) proposed by Webb and Kim (2005). The first criterion is the Variable Geometry (**VG**), where the regenerator housing cross sectional area (or housing diameter D_h) and length (L) are allowed to vary, keeping a constant housing volume. The second criterion is the Fixed Face Area (**FA**), where the regenerator housing cross sectional area is kept constant and the regenerator length can vary, thus changing also the housing volume. For reasons that will be discussed later, the Fixed Geometry (**FG**) criterion was not evaluated in this paper. The baseline (reference) housing geometry has the following geometric characteristics: $D_h = 25$ mm and $\zeta = 2$, where $\zeta = L/D_h$ is the aspect ratio of the regenerator housing. The baseline housing volume is 24.544 cm^3, and the ranges of the variables explored in the analysis are presented in Table 1.

ISSN 2176-5480

Table 1. Cases for simulation based on the PEC.

PEC	D_h range [mm]	ζ range	Housing volume (cm^3)	D_p range (mm)
VG	12.5-100	1-16	24.544	0.25-2
FA	25	1-16	Variable	0.25-2

As can be seen from Table 1, all D_h and ζ combinations in the **VG** criterion result in a housing volume of 24.544 cm^3. The particle diameter is varied from 0.25 mm to 2 mm (a realistic manufacturing range), for each possible combination. In the **FA** criterion, D_h is fixed at 25 mm, while ζ is changed from 1 to 16. The particle diameter is also varied from 0.25 mm to 2 mm for each possible combination. Additionally, for each combination of D_h, ζ and D_p, the simulations were carried out considering the constraints presented in Table 2. The physical properties of the working fluid are those of water and the solid material is assumed to have the physical properties of stainless steel. The $g(t^*)$ function that describes the fluid flow waveform was set as sinusoidal.

Table 2. Constraints of the numerical analysis and optimization.

Variable	Value or range	Units
ε	0.36	-
T_{HHEX}	283	K
T_{CHEX}	323	K
ΔT_{span}	40	K
f	1	Hz
VG - $\dot{m}$	50, 75, 100	kg/h
VG - ϕ	0.5, 0.74, 0.99	-
FA - $\dot{m}$	50, 100, 150, 200	kg/h
FA - ϕ	Variable	-

As seen from Table 2, the frequency and the temperature span were kept constant in all simulations, while the mass flow rate was varied over a certain range according to the criterion. The utilization factor, ϕ, may be constant or variable depending on whether the PEC is **VG** or **FA**. The utilization factor is defined as the ratio of the thermal masses of the fluid and solid phases,

$$\phi = \frac{c_{p,f} m_f}{c_{p,s} m_s} = \frac{c_{p,f} \dot{m}}{f c_s \rho_s (1-\varepsilon) A_c L} \tag{17}$$

The utilization factor is an important parameter in regenerator analysis, since high regeneration effectiveness is generally associated with $\phi < 1$, i.e., a large thermal mass of the regenerative matrix (Rowe *et al.*, 2005). Keeping in mind that the solid regenerative material may be one of the most expensive items of the system, the lowest possible value of utilization factor that maximizes the thermal performance should be always sought in regenerator design.

In the **VG** cases, at a fixed frequency, the utilization factor is only a function of the mass flow rate due to fixed housing volume and porosity of the packed bed of spheres. On the other hand, for the **FA** criterion, the utilization factor will decrease with ζ because the regenerative matrix mass increases with L, while the remaining parameters remain constant. Thus, in the **VG** criterion ϕ can only be changed by changing the mass flow rate, while for **FA** cases, ϕ varies with the mass flow rate and with the aspect ratio of the housing.

A fixed hot-blow regenerator effectiveness has been set as a performance constraint in the present analysis. The hot-blow effectiveness is defined as,

$$\epsilon = \frac{\dot{Q}}{\dot{Q}_{max}} = 1 - \frac{\dot{m} c_{pf} (\overline{T}_{HB} - T_{CHEX})}{\dot{m} c_{pf} (T_{HHEX} - T_{CHEX})} \tag{18}$$

where $\dot{m}$ is the average mass flow rate, $\overline{T}_{HB}$ is the average temperature of the fluid exiting the regenerator at the cold end (during the hot blow). In the **VG** and **FA** criteria, a fixed hot-blow regenerator effectiveness is equivalent to a fixed heat transfer rate when the mass flow rate and the temperatures of the sources are fixed. In the present analysis, a target value of ϵ was set at 95%. It should be noted that the fixed geometry (**FG**) PEC, i.e., that in which the regenerator length and cross-section area are kept fixed, was not evaluated in the present paper because fixing a value of ϵ in this case does not necessarily correspond to a fixed heat transfer rate.

ISSN 2176-5480

In the **VG** cases, for fixed values of mass flow rate and utilization, the regenerator effectiveness will change as a result of changes in D_h and ζ (which are reciprocal because of the constant housing volume constraint) or D_p. Changes in cross-section area affect the fluid superficial velocity, the particle Reynolds number (which is also affected by D_p) and the impact of axial heat conduction. The surface area per unit volume is directly affected by the particle diameter.

In the **FA** cases, the interstitial heat transfer coefficient is only a function of D_p, since the superficial velocity is constant for a given mass flow rate, while the interstitial area changes with both D_p and ζ. The utilization factor decreases with increasing ζ, which contributes to achieving higher values of regenerator effectiveness due to the larger thermal mass of the solid phase.

3. NUMERICAL IMPLEMENTATION

3.1 Solution of the governing equations

The solution procedure described in this section was carried out in order to calculate the regenerator entropy generation, S_g, for each operating condition defined by a set of constraints specified in Table 2. For a specific value of flow rate, the ranges of the variable parameters (e.g., housing and particle diameters, aspect ratio, etc.) were chosen according to the PEC (**VG** or **FA**) presented in Table 1.

For each condition, the governing equations for the fluid and solid phases in dimensionless form (Eqs. 3, 8 and 10) were solved using the finite volume method. The energy equations were implemented using an implicit scheme so that a coupled solution of these equations is performed at a given time. Since the momentum equation is not position-dependent, a fully explicit discretization scheme was adopted. Nevertheless, the Ergun inertial term contains a strong non-linearity, which requires an interative solution (Patankar, 1980; Maliska, 2004).

At any given time, the fluid equations are solved first and the solid energy equation is solved next. The iterative procedure is repeated until the convergence criteria are satisfied. The Weighted Upstream Differencing Scheme (WUDS) was used in the fluid energy equation and the Central Difference Scheme (CDS) was applied in the solid. The solver was based on a line-by-line method (Thomas Algorithm).

The initial conditions for the fluid and solid energy equations are linear temperature profiles, i.e. $\theta_{f,s}(z^* = 0) = 0$ and $\theta_{f,s}(z^* = 1) = 1$, to accelerate the numerical convergence. The fluid momentum equation needs only an initial condition for the fluid velocity. Thus, $u_D^*(t^* = 0) = 0$. The boundary conditions for the solid phase are $\partial\theta_s/\partial t^*(t^*, z^* = 0) = \partial\theta_s/\partial t^*(t^*, z^* = 1) = 0$. The boundary conditions for the fluid phase depend of the direction of the fluid flow. For convenience, if $u^* > 0$, then at $z^* = 0$ an open inlet boundary condition is used where fluid at T_{CHEX} enters in the matrix, and at $z^* = 1$ an open outlet is applied. On the other hand, if $u^* < 0$, an inlet is applied at $z^* = 1$ where fluid at T_{HHEX} enters in the matrix and an oulet is set at $z^* = 0$ (Maliska, 2004).

A numerical mesh consisting of 360 time steps and 200 volumes has been used. Based on preliminary numerical runs, this mesh size was proven to be satisfactory because the difference in the calculated regenerator thermal effectiveness, when compared with a mesh with 720 time steps and 400 volumes, was of the order of 0.5%, with 60% lower computing time.

After numerical convergence of the velocity and temperature fields, Eqs. (15) and (16) are used to compute the entropy generation in the regenerator, which is the objective function in the optimizations according to the **VG** and **FA** criteria.

3.2 Implementation of the PEC

After the results have been generated for a specific case (defined by the value of the flow rate and ranges of parameters associated with each PEC), the regenerator configurations that yield a predefined value of effectiveness are identified. To illustrate the analysis, Fig. 1 presents the results for PEC **FA** with $\dot{m} = 200$ kg/h. Lines of constant S_g (red lines) are plotted together with lines of constant effectiveness (blue lines), as a function of the particle diameter (x-axis) and housing aspect ratio (y-axis).

The target value of $\epsilon = 95\%$ (blue solid line) can be achieved with different combinations of ζ and D_p, with D_h and $\dot{m}$ being held constant. For small D_p, $\epsilon = 95\%$ can be achieved with small ζ because small particle diameters give rise to high values of NTU (large surface area per unit volume). As D_p increases and the interstitial heat transfer becomes poorer, it is necessary to increase the housing aspect ratio (which maintains a large heat transfer area, but decreases the utilization factor) to achieve $\epsilon = 95\%$. Along the line of constant effectiveness at 95%, different values of S_g can be verified, with a clear minimum occuring in the vicinity of a 0.5-mm particle diameter for this specific condition. Analyses similar to the one presented in Fig. 1 were carried out for all cases simulated in the present work for the **FA** and **VG** PEC.

ISSN 2176-5480

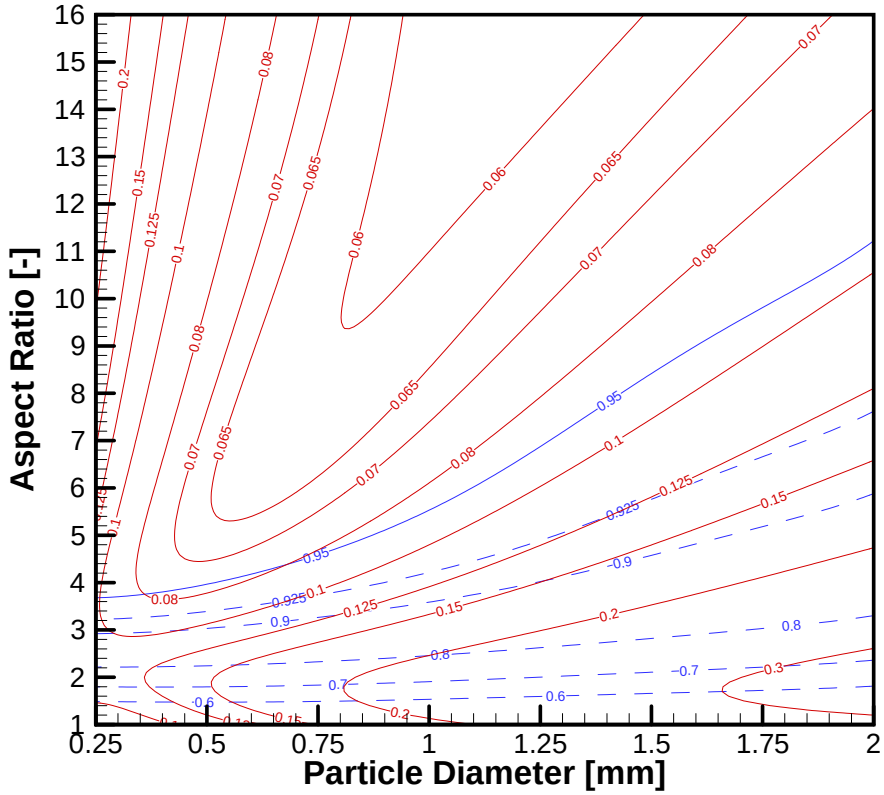

Figure 1. Effectiveness (blue lines) and S_g lines (lines) in function of the particle diameter and aspect ratio (**FA** PEC with $\dot{m} = 200$ kg/h).

4. RESULTS AND DISCUSSIONS

4.1 Contributions to the total entropy generation

This section illustrates the contributions of the three sources of entropy generation (interstitial heat transfer, axial conduction and viscous dissipation) for two regenerators with the same housing volume, but very distinct values of housing diameter and aspect ratio, as seen in Table 3. In the two cases, the particle diameter is varied between 0.25 and 2 mm. The flow rate was 100 kg/h in both cases. However, it should be noted that the simulated cases do not have the same effectiveness.

Table 3. Parameters of the case study on the contributions to the total entropy generation.

Case	D_h [mm]	ζ	D_p [mm]
Case 1	12.5	16	0.25-2
Case 2	100	0.03125	0.25-2

Figure 2 shows the total entropy generation and the individual contributions as a function of the particle diameter for Cases 1 and 2 of Table 3. Case 1 (Fig. 2.a) is a thin (small housing diameter) and long regenerator. As expected, the contributions due to axial heat conduction are very small and the total entropy generation is basically a combination of viscous dissipation (because of the long matrix length and the high superficial velocity) and interstitial heat transfer. For small particle diameters, viscous dissipation is the main source of entropy because of the large values of pressure drop. As the particle diameter increases, the pressure drop decreases but the interstitial heat transfer becomes less effective. In this way, the entropy generated due to a finite temperature difference between the solid and the fluid becomes more important. A local minimum S_g at a particle diameter of around 0.75 mm can be verified.

Case 2 (Fig. 2.b) illustrates an opposite situation, i.e., a large-diameter short regenerator, in which the contributions of axial heat conduction are expected to be more important, because of the low superficial velocity and the short regenerator length. The total entropy generation in Case 2 is a combination of the entropy production by axial heat conduction and interstitial heat transfer. As shown in Fig. 2.b, for small particle diameters, axial heat conduction in the solid is the main source of entropy generation. As the particle diameter increases, interstitial heat transfer is poorer and the dispersion in the fluid phase becomes more important. In this case, the total entropy generated is almost constant because there are

ISSN 2176-5480

three main sources of entropy production that compensate each other.

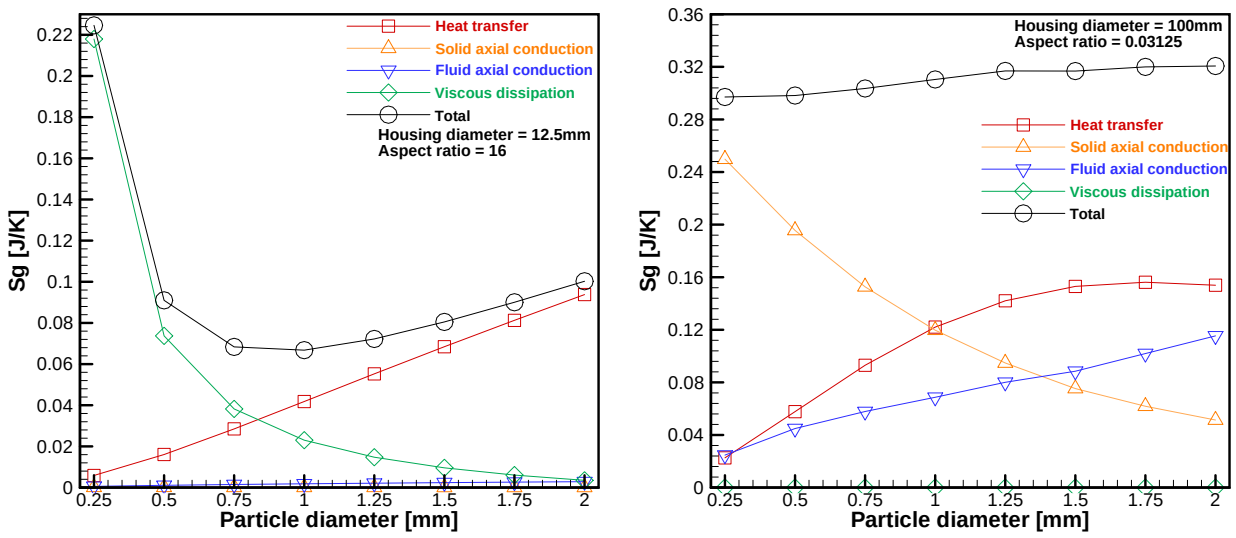

(a) (b)

Figure 2. Entropy generated by each contribution: (a) Case 1 - $D_h = 12.5$ mm and $\zeta = 16$; (b) Case 2 - $D_h = 100$ mm and $\zeta = 0.03125$.

4.2 Variable Geometry

In this section, the results for the **VG** PEC are presented as a function of the variables D_h, ζ and D_p along the line of constant 95% effectiveness. Figure 3 shows the variation of S_g as a function of D_p for mass flow rates of 50, 75 and 100 kg/h. Also, the values of D_h and ζ that correspond to the effectiveness of 95% for each D_p are also presented.

As can be seen, a minimum S_g exists for each mass flow rate, which means there are optimal values of D_p, D_h and ζ that can be combined to yield an effectiveness of 95% with a minimum entropy production. The results for the **VG** case are further illustrated in Fig. 4, which shows S_g as a function of D_p, D_h and ζ for $\dot{m} = 50$, 75 and 100 kg/h. The results shown in Fig. 4 allow the identification of optimal combinations of D_p, D_h and ζ for each mass flow rate used in the VG PEC for $\epsilon = 95\%$. A summary of these results is presented in Table 4.

Table 4. Optimized parameter ranges for the **VG** PEC.

$\dot{m}$	$D_p \times D_h \times \zeta$ range
50 kg/h	(1.12 mm × 18.5 mm × 4.94)
75 kg/h	(0.64 mm × 24.5 mm × 2.13)
100 kg/h	(0.34 mm × 30 mm × 1.16)

A deeper evaluation of the results reveals that for $\dot{m} = 50$ kg/h the optimal region involves bigger particle diameters. Therefore, as the interstitial heat transfer is less effective and the viscous losses are smaller for bigger particle diameters, long regenerative matrices with smaller housing diameters are required in order to achieve 95% regenerator effectiveness. On the other hand, for $\dot{m} = 100$ kg/h the optimized region involves small particle diameters, larger housing diameters and smaller values of aspect ratio. Since at high mass flow rates the viscous losses become more important, one needs big diameter housings (to decrease the superficial velocity) and shorter matrices. Nevertheless, the small particle diameters are necessary to improve the interstitial heat transfer and guarantee an optimal performance of the regenerator.

4.3 Fixed Frontal Area

This section presents the results for the **FA** PEC as a function of the variables ζ and D_p along the line of 95% effectiveness. Figure 5(a) shows the variations of S_g and ζ as a function of D_p for mass flow rates ranging from 50 to 200 kg/h.

The results for the **FA** PEC show that for the lower values of mass flow rate the minimum S_g region is outside the range of the simulated D_p region. However, there are minimum values of S_g for higher mass flow rates, which means that for a housing diameter of 25 mm at the highest flow rates, there are optimum values of D_p and ζ that yield an effectiveness of 95% with a minimum entropy production.

ISSN 2176-5480

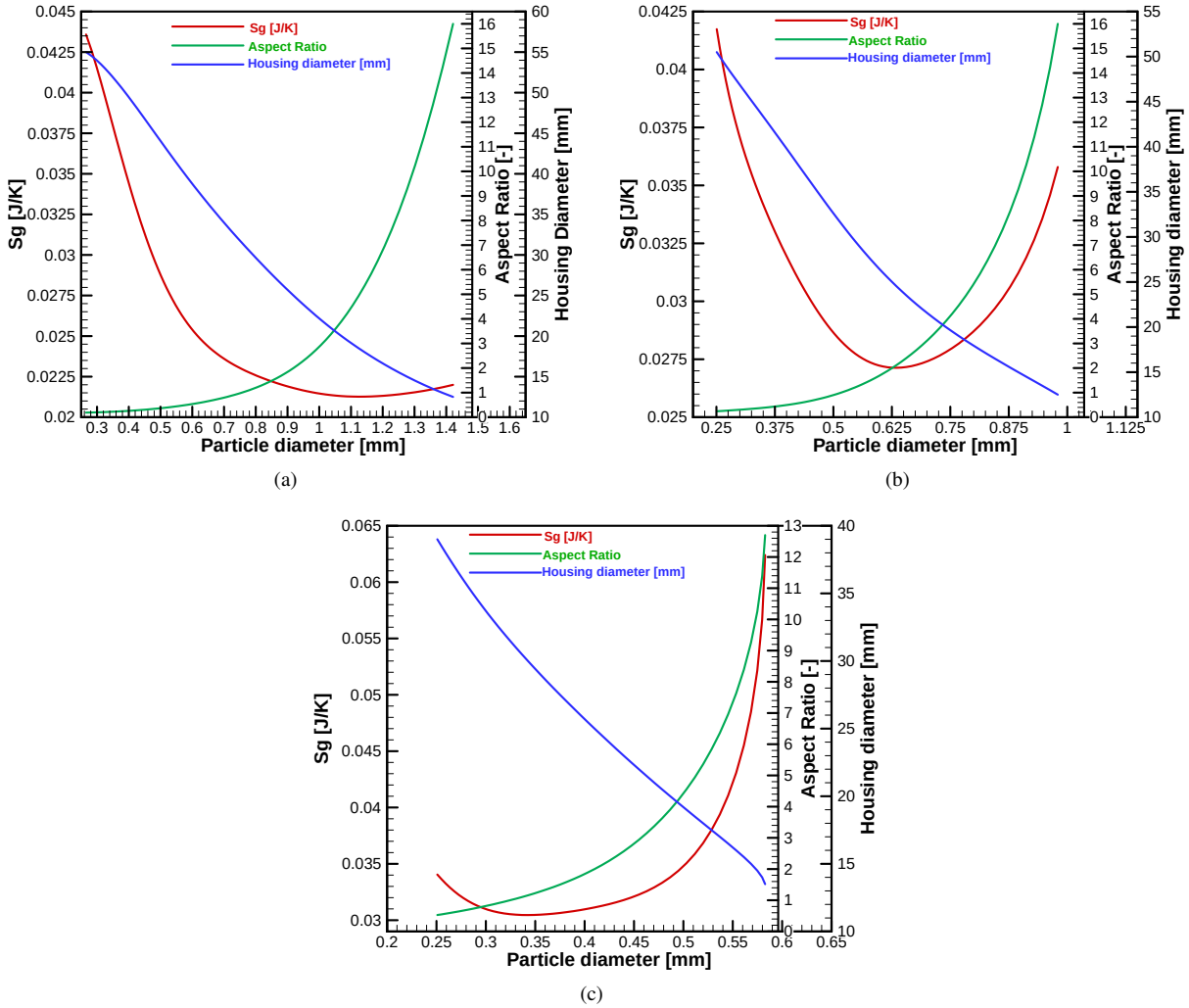

Figure 3. Entropy generated in the **VG** PEC for $\epsilon = 95\%$: (a) $\dot{m} = 50$ kg/h; (b) $\dot{m} = 75$ kg/h; (c) $\dot{m} = 100$ kg/h.

The **FA** PEC is further explored in Fig. 6, which shows S_g as a function of D_p and of ζ for mass flow rates ranging from 50 to 200 kg/h. Table 5 comprises the optimized regions for each mass flow rate.

Table 5. Optimized Optimized parameter ranges for the **FA** PEC

$\dot{m}$	$D_p \times D_h \times \zeta$ range
50 kg/h	(0.29mm $\times$ 25mm $\times$ 1)
100 kg/h	(0.25mm $\times$ 25mm $\times$ 1.8)
150 kg/h	(0.38mm $\times$ 25mm $\times$ 2.88)
200 kg/h	(0.47mm $\times$ 25mm $\times$ 3.91)

As can be seen from the results, for $\dot{m} = 50$ and 100 kg/h the optimal region seems to be located in regions of small particle diameters and small values of aspect ratio that are outside the ranges of the simulated parameters. However, because the lowest values simulated of the aspect ratio were indeed very small, it is likely that the lowest values of the calculated S_g at these mass flow rates are quite close to the minimum entropy generation values. As the aspect ratio and mass flow rates are small, losses due to axial heat conduction are expected to be the main source of entropy generation at these flow rates.

As the mass flow rate is increased, the advection term becomes more important in the energy equation and the value of NTU is decreased. Therefore, a bigger value of the regenerator length (i.e., a larger interstitial area and a lower utilization factor) is needed to keep the effectiveness at 95%. However, when ζ increases, a larger particle diameter is needed to compensate for the entropy generated due to the viscous dissipation.

ISSN 2176-5480

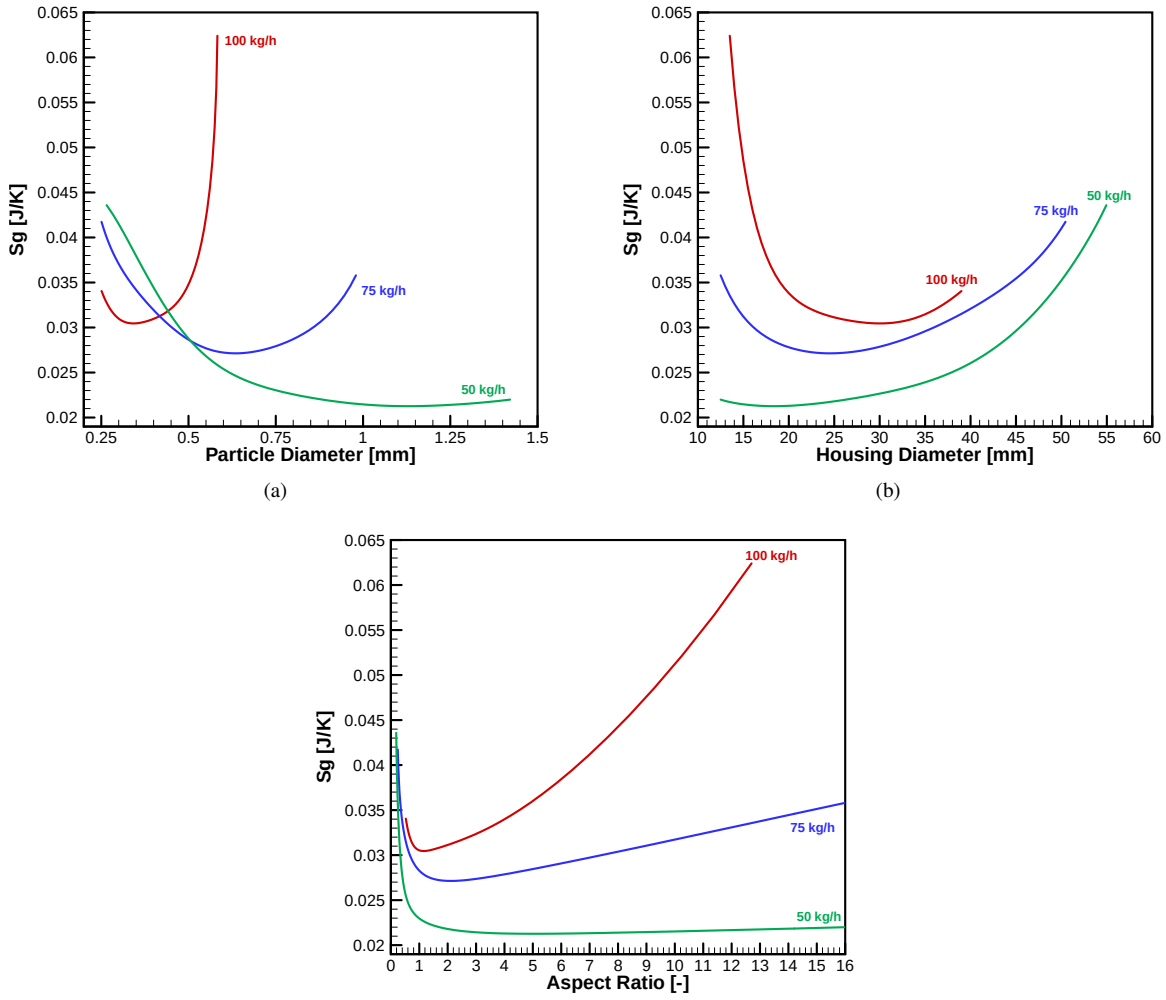

Figure 4. Minimum entropy region analysis in the **VG** PEC for $\epsilon = 95\%$ and flow rates of 50, 75 and 100 kg/h: (a) S_g as a function of D_p; (b) S_g as a function of D_h; S_g as a function of ζ.

5. CONCLUSIONS

This paper presented an optimization analysis of passive regenerators based on the Entropy Generation Minimization (EGM) method combined with a one-dimensional model for the fluid flow and coupled heat transfer in the porous regenerative matrix. Entropy generation contributions due to axial heat conduction, fluid friction and interstitial heat transfer were taken into account in the mathematical model. The model was combined with the Variable Geometry and Fixed Face Area Performance Evaluation Criteria (PEC) of (Webb and Kim, 2005) to determine optimal regenerator configurations subjected to constant effectiveness constraints. The influence of parameters such as the mass flow rate, regenerator cross sectional area, housing aspect ratio, utilization factor and particle diameter was investigated, and ranges of optimal values of these parameters have been identified.

6. ACKNOWLEDGEMENTS

The authors thank the CNPq for financial support through grant No. 573581/2008-8 (National Institute of Science and Technology in Cooling and Thermophysics). Financial support from Embraco is also acknowledeged.

7. REFERENCES

Awad, M.M. and Muzychka, Y.S., 2012. *Thermodynamic Optimization*, INTECH, chapter 1, pp. 3–52.

Bejan, A., 1982. *Entropy Generation through Heat Transfer and Fluid Flow*. Wiley.

Bejan, A., 1996. *Entropy Generation Minimization: The Method of Thermodynamic Optimization of Finite-Size Systems and Finite-Time Processes*. CRC Press.

ISSN 2176-5480

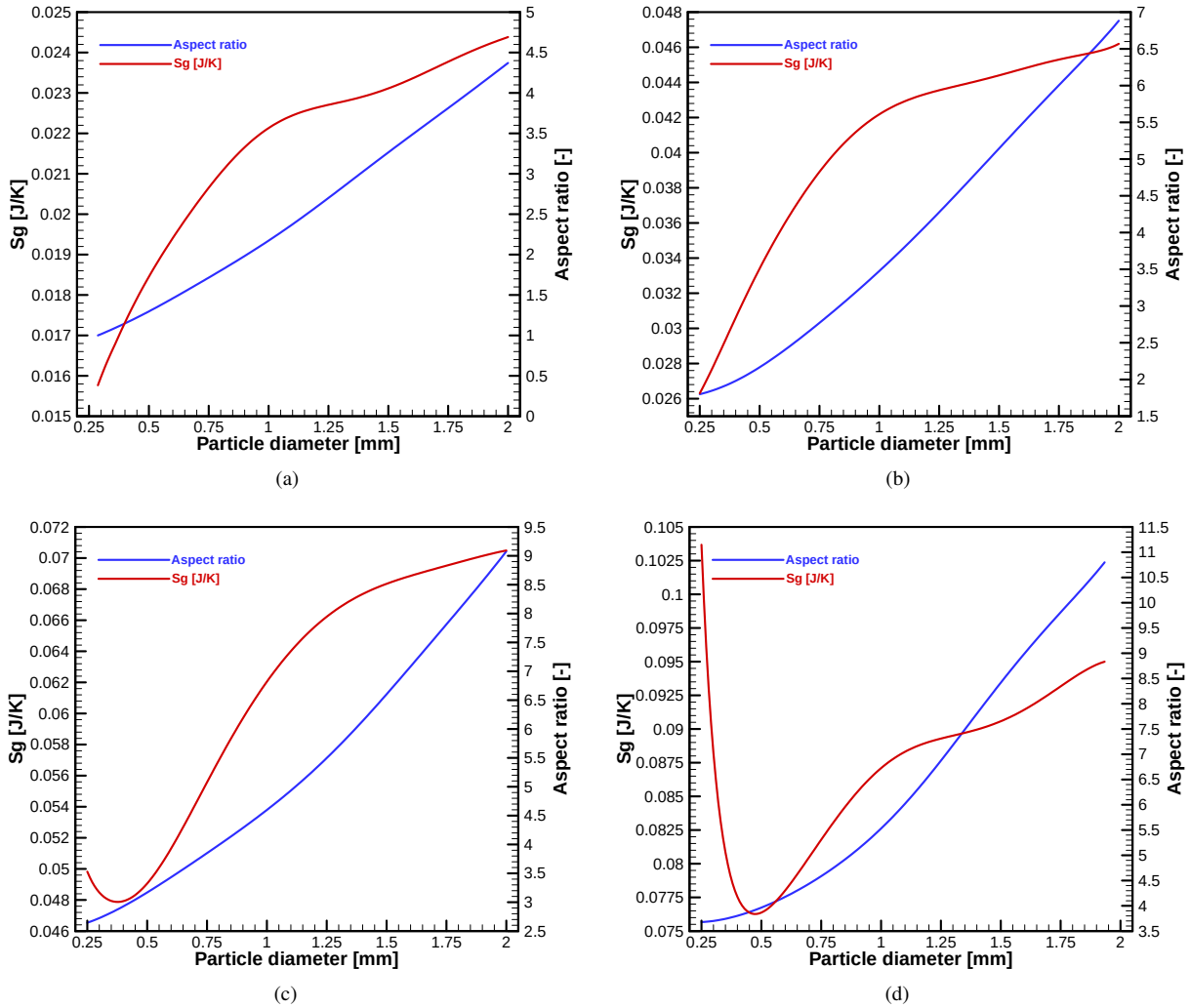

Figure 5. Entropy generated in the **FA** PEC for $\epsilon = 95\%$: (a) $\dot{m} = 50$ kg/h; (b) $\dot{m} = 100$ kg/h; (c) $\dot{m} = 150$ kg/h; (d) $\dot{m} = 200$ kg/h.

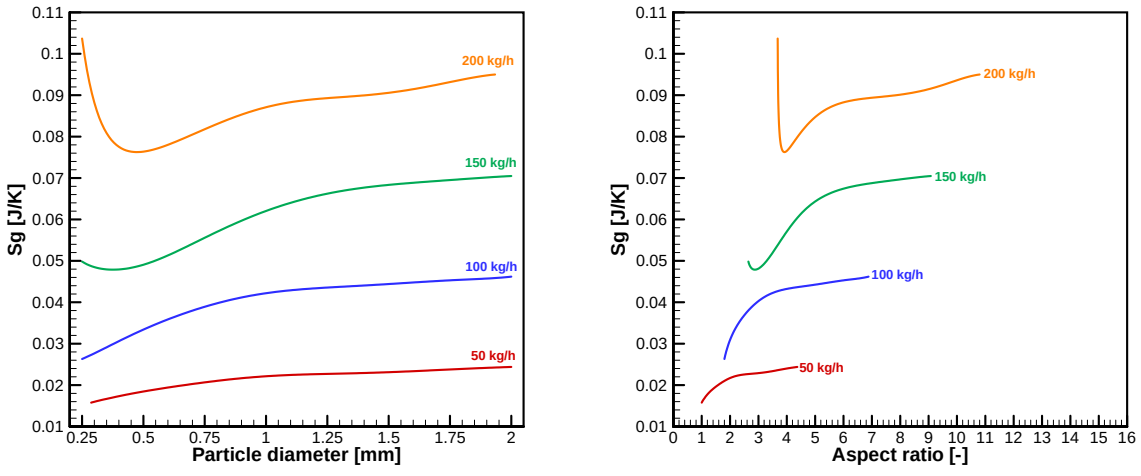

Figure 6. Minimum entropy region analysis in the **FA** PEC for $\epsilon = 95\%$ and flow rates of 50, 75, 100 and 200 kg/h: (a) S_g as a function of D_p; (b) S_g as a function of ζ.

Das, S.K. and Sahoo, R.K., 1991. "Thermodynamic optimization of regenerators." *Cryogenics*, Vol. 31, pp. 862–868.
Das, S.K. and Sahoo, R.K., 1999. "Second law analysis of a cyclic regenerator in presence of longitudinal heat conduction

ISSN 2176-5480

in matrix." *Heat and Mass Transfer*, Vol. 34, pp. 395–403.

de Waele, A.T.A.M., Steijaert, P.P. and Gijzen, J., 1997. "Thermodynamical aspects of pulse tubes". *Cryogenics*, Vol. 37, pp. 313–324.

Hadley, G.R., 1986. "Thermal conductivity of packed metal powder". *International Journal of Heat and Mass Transfer*, Vol. 29, pp. 909–920.

Kaviany, M., 1995. *Principles of Heat Transfer in Porous Media*. Springer, 2nd edition.

Kaviany, M., 2002. *Principles of Heat Transfer*. John Wiley & Sons.

Koch, D.L. and Brady, J.F., 1985. "Dispersion in fixed beds". *Journal of Fluid Mechanics*, Vol. 154, pp. 399–427.

Krane, R.J., 1987. "A second law analysis of the optimum design and operation of thermal energy storage systems". *International Jounal of Heat and Mass Transfer*, Vol. 30, pp. 43–57.

Maliska, C.R., 2004. *TransferÃČÂłncia de Calor e MecÃČÂćnica dos Fluidos Computacional*. LTC, 2nd edition.

Nam, K. and Jeong, S., 2006. "Development of parallel wire regenerator for cryocoolers". *Cryogenics*, Vol. 46, pp. 278–287.

Nield, D.A. and Bejan, A., 2006. *Convection in Porous Media*. 3rd edition.

Oliveira, P.A., Trevizoli, P.V., Barbosa, Jr., J.R. and Prata, A.T., 2012. "A 2D hybrid model of the fluid flow and heat transfer in a reciprocating active magnetic regenerator". *International Journal of Refrigeration*, Vol. 35, pp. 98–114.

Patankar, S.V., 1980. *Numerical Heat Transfer and Fluid Flow*. Hemisphere Publishing Corporation.

Pecharsky, V.K. and Gschneidner, Jr., K.A., 1999. "Magnetocaloric effect and magnetic refrigeration". *Journal of Magnetism and Magnetic Materials*, Vol. 200, pp. 44–56.

Pussoli, B.F., J R Barbosa, J., da Silva, L.W. and Kaviany, M., 2012. "Optimization of peripheral finned-tube evaporators using entropy generation minimization". *International Journal of Heat and Mass Transfer*, Vol. 55, pp. 7838–7846.

Rowe, A., Tura, A., Dikeos, J. and Chahine, R., 2005. "Near room temperature magnetic refrigeration". In *Proceedings in International Green Energy Conference*. Ontario, Canada.

Schmidt, F.W. and Willmott, A.J., 1981. *Thermal Energy Storage and Regeneration*. Hemisphere Publishing Co.

Shah, R.K. and Sekulic, D.P., 2003. *Fundamentals of Heat Exchanger Design*, Wiley.

Steijaert, P.P., 1999. *Thermodynamical aspects of pulse-tube refrigerators*. Ph.D. thesis, Technical University of Eindhoven.

Trevizoli, P.V., Barbosa Jr., J.R., Tura, A., Arnold, D. and Rowe, A., 2013. "Modeling of thermo-magnetic phenomena in active magnetic regenerators". In *Proceedings of the of the ASME 2013 Summer Heat Transfer Conference*. HT 2013 Minneapolis, USA.

Trevizoli, P.V., J R Barbosa, J., de Oliveira, P.A., Canesin, F.C. and Ferreira, R.T.S., 2012. "Assessment of demagnetization phenomena in the performance of an active magnetic regenerator". *International Journal of Refrigeration*, Vol. 35, pp. 1043–1054.

Webb, R.L. and Kim, N.H., 2005. *Principles of Enhanced Heat Transfer*. Taylor & Francis, 2nd edition.

Zhao, T. and Cheng, P., 1996. "Oscillatory heat transfer in a pipe subjected to a laminar reciprocating flow". *ASME Journal of Heat Transfer*, Vol. 118, pp. 592–598.

Zhao, T.S. and Cheng, P., 1998. "Heat transfer in oscillatory flows". In *Annual Review of Heat Transfer*, Begell House.

8. RESPONSIBILITY NOTICE

The authors are the only responsible for the printed material included in this paper.